INSTITUTO DE PESQUISAS TECNOLÓGICAS

COMUNICAÇÃO TÉCNICA

Nº 179543

The use of FactSageTM to determine crystalline phases in blast furnace slag based glass

Catia Fredericci

Artigo publicado no Engenharia, gestão e inovação. Belo Horizonte: Editora Poisson, 2025. v.18. Cap. 11, p.191-202.

"Comunicação Técnica" compreende trabalhos elaborados por técnicos do IPT, apresentados em eventos, publicados em revistas especializadas ou quando seu conteúdo apresentar relevância pública. **PROIBIDO REPRODUÇÃO**

Instituto de Pesquisas Tecnológicas do Estado de São Paulo S/A - IPT
Av. Prof. Almeida Prado, 532 | Cidade Universitária ou
Caixa Postal 0141 | CEP 01064-970
São Paulo | SP | Brasil | CEP 05508-901
Tel 11 3767 4374/4000 | Fax 11 3767-4099

www.ipt.br

Capítulo 11

The use of FactSageTM to determine crystalline phases in blast furnace slag-based glass ceramic

Cátia Fredericci

Abstract: FactSage™ is a thermodynamic simulation software widely utilized in both industry and academic institutions, including universities and research centers. It is particularly effective for calculating properties and equilibria of complex chemical systems, especially in high-temperature phase equilibria, which are relevant to the metallurgy and ceramics industries. This work aimed to employ FactSage to determine the crystalline phases developed during the crystallization of glass made from blast furnace slag. The glasses were produced by melting and quenching a mixture of blast furnace slag (80% and 60% by weight) and soda-lime-silica glass (20% and 40% by weight). After the resulting glasses were heat-treated, the developed crystalline phases were analyzed using X-ray diffraction. These results were then compared to those obtained through computational simulation. The findings indicated that FactSage is a promising tool for designing glass ceramics.

Keywords: glass-ceramic, slag, cullet, FactSage, thermodynamic simulation.

1. INTRODUCTION

The volume of blast furnace slag produced can vary, but it is significant; approximately 270 kg of slag is generated for each ton of pig iron produced[1]. In Brazil, around 26 million tons of pig iron were produced in 2023, resulting in an estimated 7 million tons of blast furnace slag[2]. This creates a pressing need for efficient exploitation of slag, which is important for both economic opportunities and environmental management. While most of the blast furnace slag generated in Brazil is utilized in cement and concrete production[3], a surplus can be applied to other uses. Rawlings et al.[4] reported that blast furnace slag was the first silicate waste studied as a potential source material for glass ceramic in building applications. Research efforts in Brazil and around the world have focused on exploring the potential of slag for glass-ceramic production [5-10]. Glass-ceramics are polycrystalline materials created either through controlled nucleation and crystallization of monolithic glass or by sintering and crystallization of glass powder[11]. Fredericci et al.[5] investigated the crystallization and properties of glass and glass ceramics made from 100% blast furnace slag sourced from CSN (Companhia Siderúrgica Nacional – Volta Redonda, Brazil). They found that melilite (a solid solution of gehlenite [$Ca_2Al_2SiO_7$] and akermanite [$Ca_2MgSi_2O_7$]) was the main crystalline phase present in the glass-ceramic. According to the latest survey by the Technical Association of Brazilian Glass (ABIVIDRO), approximately 47% of glass is recycled in Brazil[12]. Considering the annual production of 3.2 million tons of hollow and flat glass[13], and the low rate of glass recycling in the country, combining blast furnace slag with recycled glass presents a valuable opportunity for producing glass ceramics.

2. EXPERIMENTAL

2.1. RAW MATERIALS, MELTING, AND CHEMICAL ANALYSIS

The glass was produced by melting a mixture of slag from USIMINAS (Minas Gerais, Brazil) and cullet (soda-lime-silica glass from bottles), in the proportions shown in Table 1. To remove metallic iron from the slag, magnetic separation was utilized. Both the slag and glass powder had a particle size of less than 100 mesh (150 μm). Batches weighing 50 grams were melted in a homemade alumina-magnesia (AMS) spinel crucible. The compositions of the slag, cullet, and glass were determined using X-ray fluorescence (XRF) with a Philips Analytical XRF apparatus.

Table 1 – Compositions of slag and cullet mixtures (wt%), temperature and time of melting.

Glass	Slag (%)	Cullet (%)	Temperature (°C)	Time (h)
80S20C	80	20	1350	2
60S40C	60	40	1350	2

2.2. COMPUTATIONAL SIMULATION USING FACTSAGE

FactSage 6.4 was utilized to calculate the viscosity of glasses obtained from three different compositions: 100 wt% slag (100S), 80S20C, and 60S40C, as detailed in Table 1. The glasses database was used because it is applicable over the entire temperature range, including temperatures at and below the glass transition temperature. Additionally, thermodynamic calculations were performed using FactSage™ to predict the phases that

would form during solidification, employing the FToxid database and selecting the liquid solution FToxid_SLAGA.

2.3. DIFFERENTIAL THERMAL ANALYSIS (DTA)

The resulting glasses were analyzed using differential thermal analysis (DTA) with a Netzsch model 402 to determine the glass transition temperature (T_g) and crystallization temperature (T_c) for powder samples with a particle size between 170 mesh and 100 mesh. Approximately 100 mg of glass was placed in a platinum crucible, and the analysis was conducted at a heating rate of 20 °C/min.

2.4. HEAT TREATMENT SCHEDULE

Glass samples measuring approximately (1 x 1) cm were sanded using silicon carbide (SiC) water slurries on flat brass tools. They were then polished to an optical grade with cerium oxide slurry. The polished samples underwent heat treatment in the air atmosphere in an electric furnace, first at 720 °C for 1 hour to promote nucleation, followed by exposure to 870 °C for 20 minutes for crystal growth.

2.5. SCANNING ELECTRON MICROSCOPY

The samples were immersed in a solution of 0.2 vol% HF (48 wt%) for 20 seconds to reveal the crystalline phase developed on the surface of the glass ceramic. After removal from the solution, the samples were rinsed first with water and then with acetone, dried at 80 °C for 30 minutes, and coated with gold for analysis using a JEOL 6300 scanning electron microscope (SEM). Additionally, one sample of 80S20C glass that had been heat-treated at 870 °C for 2 h was cut, and its cross-section was analyzed by SEM.

2.6. X-RAY DIFFRACTION

To investigate the crystalline phases corresponding to the peaks in the DTA thermogram, the powdered glasses were heat-treated at the temperatures indicated by the exothermic peaks in the DTA curve, with a heating rate of 20 °C/min. Once the desired temperature was reached, the samples were immediately removed from the furnace and allowed to cool to room temperature. The crystalline phases were identified using an X-ray powder diffractometer (Shimadzu XRD 6000), employing cobalt Kα radiation.

3. RESULTS AND DISCUSSION

3.1. GLASS MELTING AND GLASS COMPOSITION

Varshynea and Mauro [14] noted the significance of viscosity (η) in glass manufacturing processes, identifying four standard viscosity reference points commonly used: the working point (10^3 Pa.s), the softening point ($10^{6.5}$ Pa.s), the annealing point (10^{12} Pa.s), and the strain point ($10^{13.5}$ Pa.s). Additionally, the viscosity at the melting point is typically below 10 Pa.s. To determine the appropriate temperature for melting glasses with nominal compositions of 80S20C and 60S40C, the viscosity concerning temperature was calculated using FactSage 6.4. The results are illustrated in Figure 1. Both glasses were

melted at 1350 °C, as the calculations indicated that the viscosity at this temperature is below 10 Pa.s, ensuring effective refining and suitable viscosity for pouring the glass into a stainless steel mold. The glass pieces obtained were then annealed at 700 °C (with viscosity around 10^{12} Pa.s, as shown in Figure 1) for 30 minutes to eliminate residual stress. As will be discussed in the next section, this temperature is closely correlated with results obtained from differential thermal analysis (DTA). Interestingly, while the viscosity of the 60S40C glass is higher at elevated temperatures compared to the 80S20C glass, the composition of the 60S40C glass contains a greater amount of Na_2O - a potent glass modifier that breaks Si-O-Si bonds - and typically reduces the viscosity of silicate melts. However, this is counteracted by an increase in the SiO_2 content and a decrease in other glass modifiers, such as CaO and MgO, in the 60S40C composition.

Figure 1 – Viscosity of the slag, glass 80S20C and 60S40C determined by FactSage™ 6.4.

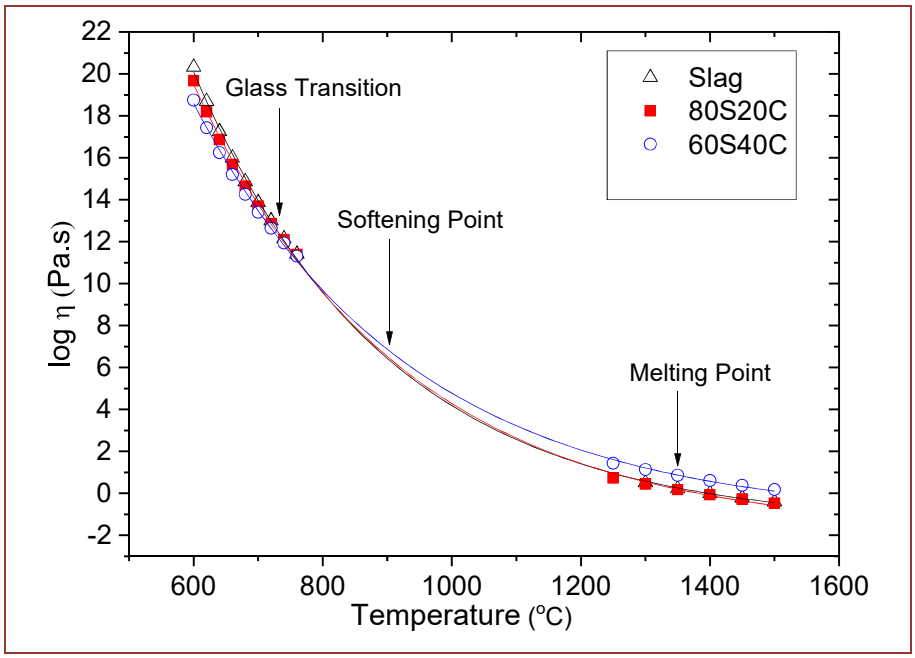

The selection of refractory materials is a critical step in the glass melting process. Since the slag contains more CaO and MgO than SiO_2 and Al_2O_3, it tends to be alkaline, which can cause corrosion of the commonly used AZS (Al_2O_3-ZrO_2-SiO_2) refractories in the glass industry. Fredericci and Morelli [15] conducted a study on the corrosion of AZS and AZ (Al_2O_3-ZrO_2) crucibles after melting a nominal 80S20C glass composition at 1360 °C for 2 hours. They found a corrosion interface between the glass and both refractory materials. Additionally, Li et al. [8] reported extensive corrosion experiments on electrocast AZS refractories using molten CaO-Al_2O_3-SiO_2. In the present work, the glass was melted in a homemade alumina-magnesia crucible to minimize glass corrosion as much as possible. As shown in Table 2, the 80S20C glass composition exhibited 9.78 wt% Al_2O_3 and 6.43 wt% MgO, compared to the nominal composition of 8.94 wt% Al_2O_3 and 5.94 wt% MgO, indicating slight corrosion of the crucible. In contrast, the composition of the 60S40C glass after melting was similar to the nominal one, suggesting that the MgO-Al_2O_3 crucible was suitable for melting this type of glass.

Table 2 – Chemical analysis of the slag (S), cullet (C), nominal and measured compositions of the glasses 80S20C and 60S40C (wt%).

Oxides	Slag (S)	Cullet(C)	80S20C		60S40C	
			Nominal	Measured	Nominal	Measured
CaO	42,33	11,20	36,10	35,11	29,88	29,71
SiO_2	36,94	72,80	44,60	44,27	51,28	51,77
Al_2O_3	10,64	2,13	8,94	9,78	7,23	6,99
MgO	7,38	0,16	5,94	6,43	4,49	4,56
Fe_2O_3	0,31	0,04	0,27	0,24	0,20	0,19
TiO_2	0,89	0,01	0,71	0,71	0,53	0,52
MnO	0,52	0,0	0,42	0,41	0,31	0,30
K_2O	0,46	0,09	0,38	0,39	0,32	0,29
Na_2O	0,34	13,20	2,89	2,45	5,48	5,39

3.2. DTA ANALYSES

Figure 2 presents the DTA curves obtained from the glasses, while Table 3 lists the characteristic temperatures derived from these curves. For the 80S20C glass, there is an inflection point at about 710 °C, which corresponds to the glass transition temperature (T_g). Additionally, an exothermic peak at 945 °C is attributed to crystallization (T_c), and an endothermic peak at 1254 °C is associated with the melting of certain crystal phases (T_m). The DTA trace for the 60S40C glass exhibits similar behavior; however, both the Tg (670 °C) and Tc (884 °C) are shifted to lower temperatures. Relating the decrease in T_g to these complex glass compositions is not straightforward. As shown in Figure 1, adding cullet to the slag reduces viscosity within the low-temperature range of 600 °C to 760 °C, with the 60S40C glass exhibiting a lower viscosity. It is important to note that the glass transition temperature is not a fixed value; it varies based on the measurement technique and heating rate used. The temperature at which the viscosity reaches 10^{12} Pa·s, as calculated by FactSage 6.4, is approximately 720 °C, which is close to the values calculated for the glasses studied in this work.

Table 3 – Typical temperatures of the DTA curves, where T_g is the glass-transition temperature, T_c is the crystallization peak temperature, and T_m is the melting point of crystalline phases.

Glass	T_g (°C)	T_c (°C)	T_m (°C)
80S20C	710	945	1254
60S40C	690	884	1220

Figure 2 – DTA curves of the powdered glass samples (-100 + 170) mesh.

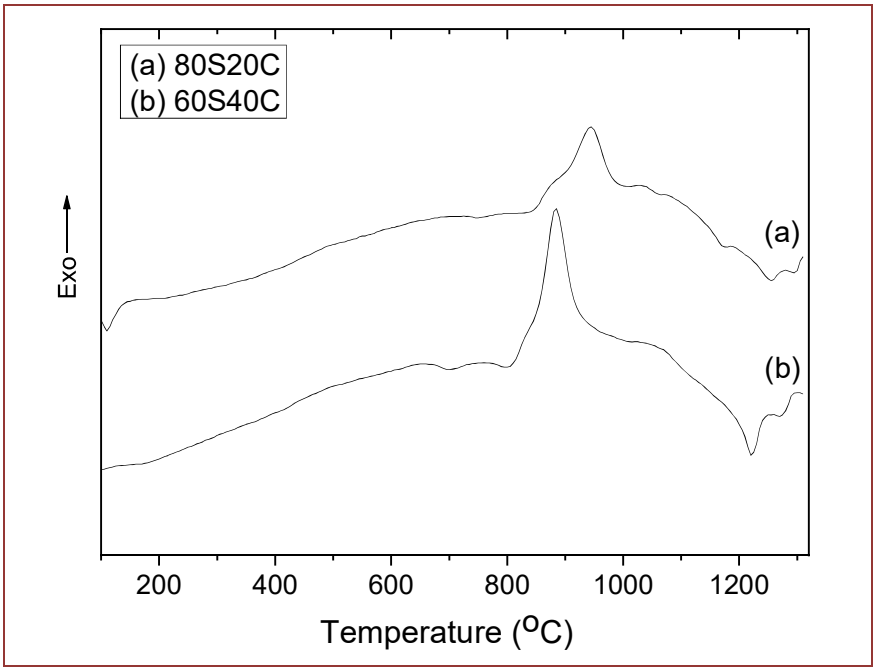

3.3. GLASS CRYSTALLIZATION

Samples of the as-quenched glass were heat-treated at 720 °C for 1 hour for nucleation, followed by treatment at 870 °C for 20 minutes to promote crystal growth. These temperatures were selected because they fall between the glass transition temperature (T_g) and the maximum peak temperature (T_c), which are 945 °C and 884 °C for the 80S20C and 60S40C glasses, respectively. Figures 2 and 3 show micrographs obtained through scanning electron microscopy (SEM) for both glass compositions. Crystals developed only on the surface of the heat-treated samples; no crystals were observed in the bulk material, even after extended treatment times at 720 °C for 20 hours, followed by 870 °C for 2 hours. It has been reported that Fe_2O_3 and TiO_2 are commonly used as nucleating agents for alumino-silicate glass ceramics, facilitating volume crystallization. However, the quantities of these oxides present in the glass compositions studied (as shown in Table 2) were insufficient to act as effective nucleating agents. Figure 2b presents SEM micrograph of a cross-section of a sample of the 80S20C glass, which was heat-treated at 870 °C for 2 h. It shows that dendritic crystals grew from the surface into the volume, but no crystals formed within the bulk of the glass. These observations are consistent with the results from differential thermal analysis (DTA), which indicated broad crystallization temperature peaks, suggesting that the surface crystallization process was predominant [16]. For the surface-crystallized 80S20C glass, the dominant crystal morphology was spherulitic-dendritic, with small rectangular crystals forming as a minority phase. In contrast, for the 60S40C glass, larger rectangular crystals were observed compared to those in the 80S20C crystallized glass.

Figure 3 - (a) SEM micrographs of the surface of the glass 8020C treated at 720 °C/ 1h and 870 °C/20 min and (b) cross-section of one sample of the same composition but heat-treated at 870 °C/1h.

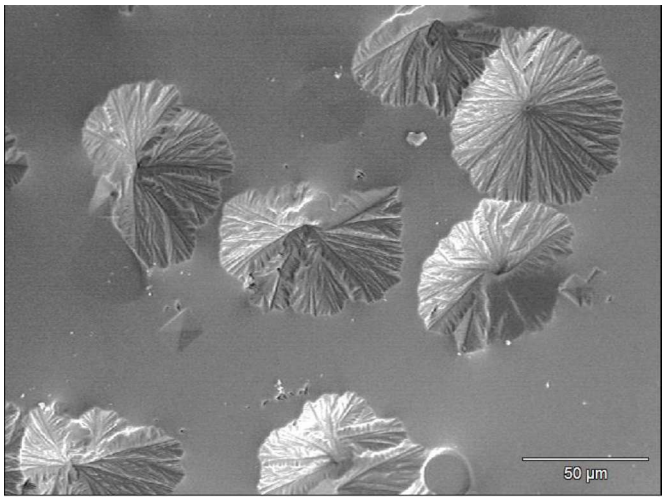

(a)

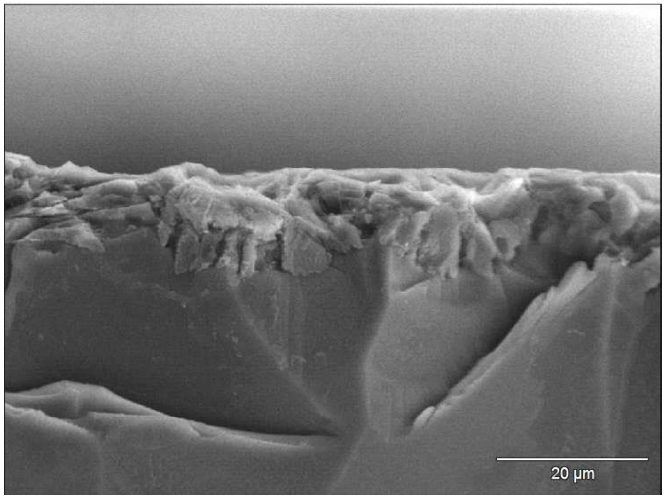

(b)

Figure 4 - SEM micrographs of the surface of the glass 60S40C treated at 720 °C/ 1h and 870 °C/20 min.

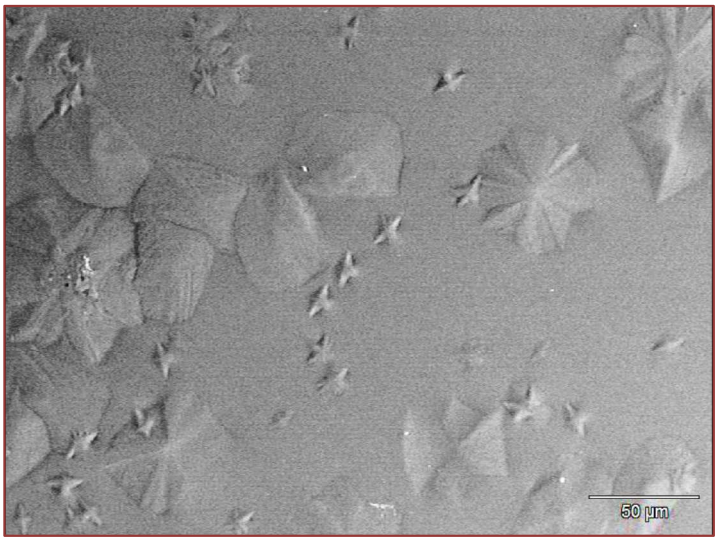

Figure 5 illustrates the simulation of the solidification of blast-furnace slag glass based on thermodynamic equilibrium. At 1350 °C, the system remains in a liquid state, confirming the temperature used to melt the glass. The first phase to develop is melilite, a solid solution of gehlenite ($Ca_2Al_2SiO_7$) and akermanite ($Ca_2MgSi_2O_7$). This is followed by merwinite ($CaMgSi2O_8$), which is metastable, as observed by Fredericci et al. [6]. The thermodynamic simulation for the glass composition 80S20C (Figure 6) indicates that melilite continues to be the major crystalline phase, but is accompanied by wollastonite (β-$CaSiO_3$). This shift occurs due to a decrease in the amounts of aluminum and magnesium - elements essential for the formation of melilite - as soda-lime-silica glass is added to the slag. It is also noteworthy that the high-temperature phase of wollastonite, α-$CaSiO_3$, transforms into β-$CaSiO_3$ (WOLL) at lower temperatures [17]. The predominance of these phases is confirmed in the diffractogram of the 80S20C glass heat-treated at 820 °C (Figure 8), aligning with the results obtained from the computational simulation. Minor phases such as nepheline ((Na, K)$AlSiO_4$) and cPyrA (pyroxene) were not identified in the diffractogram, potentially due to their low abundance during heat treatment or because the temperature and duration (820 °C for 20 minutes) were insufficient for their formation in the glass-ceramic. It is essential to emphasize that the computational simulations conducted using FactSage consider only thermodynamic parameters, not kinetic ones. As the amount of soda-lime-silica glass increases in the blast furnace slag, resulting in the composition 60S40C (Figure 7), melilite disappears as a crystalline phase (below 1030 °C), leaving wollastonite as the dominant phase at low temperatures. Other phases such as cPyrA, nepheline, and NCSO (devitrite – $Na_2Ca_3Si_6O_{16}$) were absent for the reasons mentioned above.

Figure 5 - Thermodynamic simulation of blast furnace slag solidification performed using FactSage™ software version 6.4

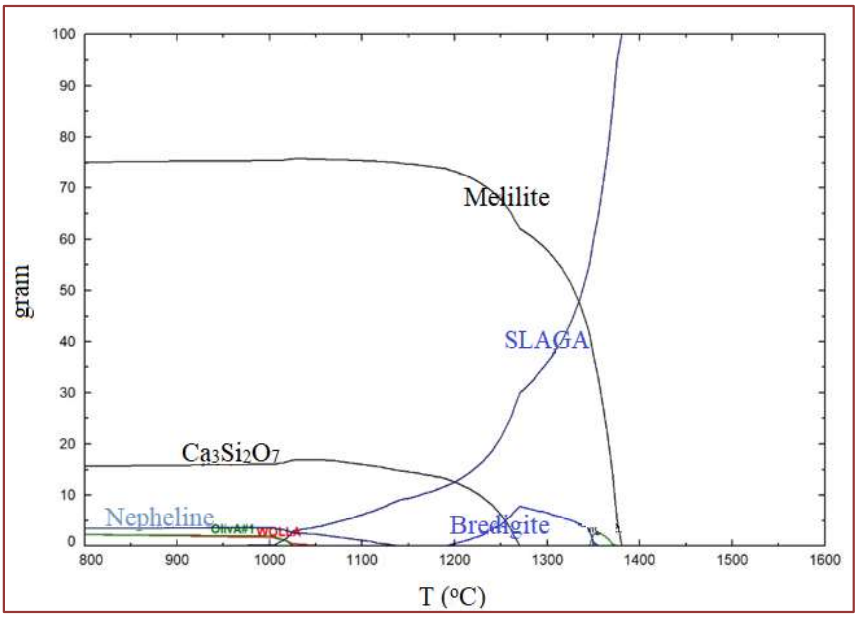

Figure 6 - Thermodynamic simulation of 80S20C solidification performed using FactSage™ software version 6.4

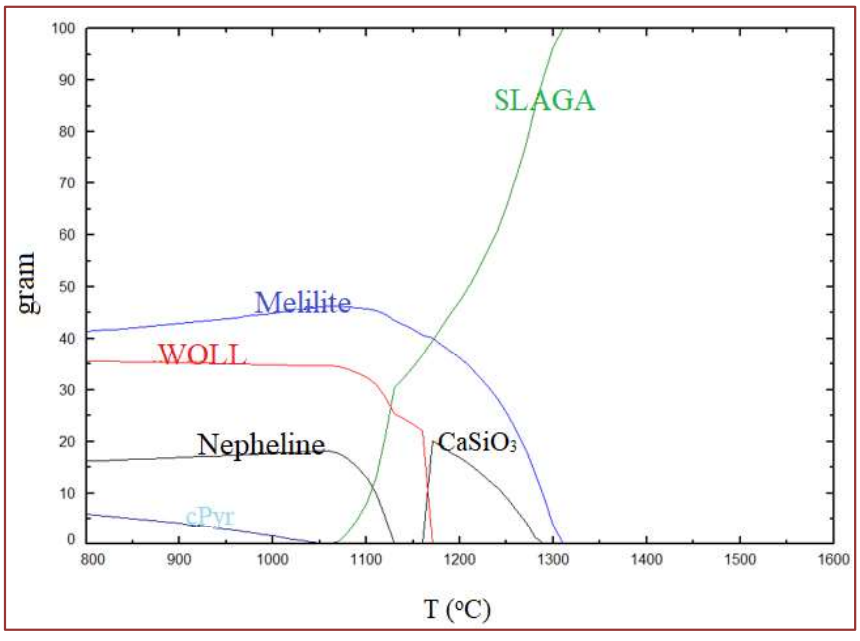

Figure 7 - Thermodynamic simulation of 60S40C solidification performed using FactSage™ software version 6.4

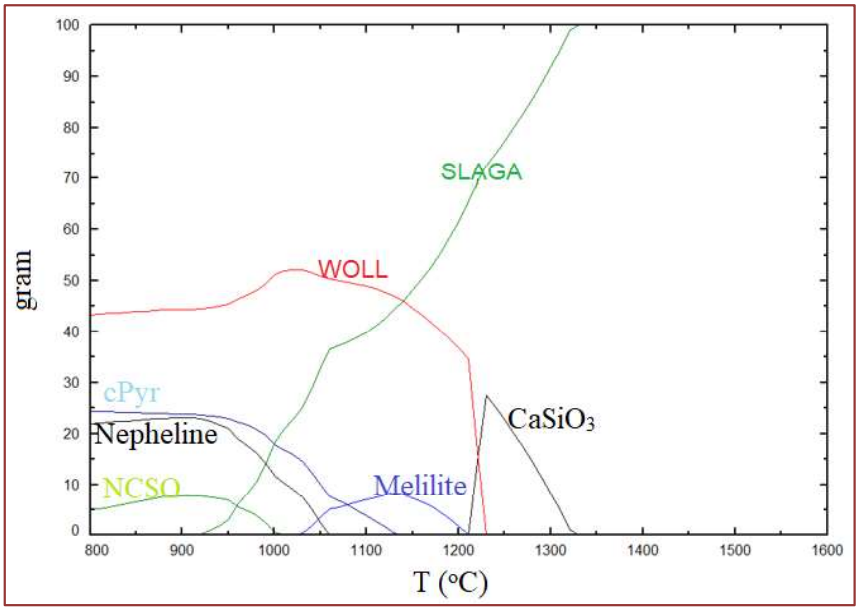

Figure 8 - X-ray diffractograms of the powdered glass 80S20C and 60S40C heat-treated at 870 °C/20 min. Cobalt Kα radiation.

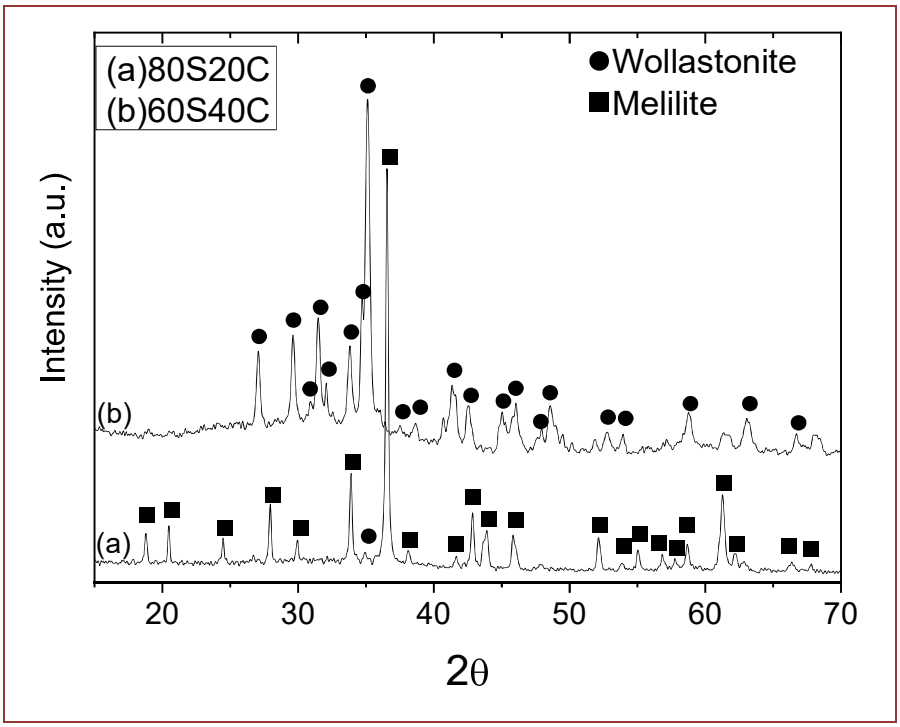

4. CONCLUSIONS

Glass and glass-ceramic were successfully produced from blast furnace slag and soda-lime silica glass. Differential thermal analysis (DTA) and scanning electron microscopy revealed that the glasses experienced heterogeneous surface crystallization. Notably, the primary crystalline phase shifted from melilite to wollastonite as the proportion of glass cullet in the composition increased. This finding was determined using FactSage and confirmed through X-ray diffraction analysis.

ACKNOWLEDGMENT

The author expresses gratitude to Tiago Ramos Ribeiro for his assistance with FactSage and to USIMINAS for donating blast furnace slag.

REFERENCES

[1] IEA – Part of the Energy Technology Perspectives Series - Iron Steel Technology Road map – Towards more sustainable steel making, 2020, 1-190 – **https://www.oecd.org/content/dam/oecd/en/publications/reports/2020/10/iron-and-steel-technology-roadmap_040b14d5/3dcc2a1b-en.pdf,** accessed on January 2025.

[2] https://www.acobrasil.org.br/site/wp-content/uploads/2024/07/Anuario_Completo_2024.pdf Accessed on January 2025.

[3] Carvalho Filho, P.A. – Escória de alto-forno – Arcellor Mitall https://brasil.arcelormittal.com/produtos-solucoes/coprodutos/coprodutos/escoria-alto-forno#:~:text=Devido%20ao%20seu%20grande%20potencial,fabrica%C3%A7%C3%A3o%20do%20cimento%20e%20concreto. Accessed on January 2025.

[4] Rawling R. D., Wu J. P., Boccaccini A. R. Glass-ceramic: The production from wastes – A review. Journal of Materials Science, 2006, 41, 733-761. doi.org/10.1007/s10853-006-6554-3.

[5] Fredericci C., Ziemath E., Zanotto E.D. Crystallization mechanism and properties of a blast furnace slag glass**.** Journal of Non-Crystalline Solids, 273, 1–3, 2000, 64-75. doi.org/10.1016/S0022-3093(00)00145-9

[6] Fredericci C., Pizani P. S., Morelli M. R. Crystallization of blast furnace slag glass melted in SnO_2 crucible J. Non-Cryst. Solids, 2007, 353, 406. doi.org/10.1016/j.jnoncrysol.2007.06.027

[7] Valderrama D.M.A, Cuaspud J.A.G, Roether J.A., Boccaccini. A.R. Development and characterization of glass ceramics from combinations of slag, fly ash, and glass cullet without adding nucleating agents. Materials, 12, 2019, 2032. doi:10.3390/ma12122032

[8] Li M., Zheng F., Xiao Y., Guan Y., Wang J., Zhen Q, et al. Utilization of residual heat to prepare high-performance foamed glass-ceramic from blast furnace slag and its reinforce mechanism. Process Safety and Environmental Protection, 156, 2021, 391-404. doi.org/10.1016/j.psep.2021.10.019

[9] Ding L., Ning W, Wang Q., Shi D., Luo. Preparation and characterization of glass–ceramic foams from blast furnace slag and waste glass. Materials Letters, 141, 2015, 327-329. doi: 10.1016/j.matlet.2014.11.122

[10] Jia R., Deng L, Yun F., Li H. Zhang X. Jia X. Effects of SiO_2/CaO ratio on viscosity, structure, and mechanical properties of blast furnace slag glass ceramics. Materials Chemistry and Physics, 233, 2019, 155–162. doi.org/10.1016/j.matchemphys.2019.05.065

[11] McMillan P.W. Glass-Ceramics, second ed., Academic Press: New York, 1979.

[12] https://www.reciclasampa.com.br/artigo/governo-federal-cria-sistema-nacional-para-reciclagem-de-vidro, accessed on January 2025.

[13] Zampelli, C. Panorama da Indústria Brasileira de Vidro – Associação Brasileira das Indústrias de Vidro – II Workshop Universidade/Indústria em Materiais Vítreos – São Carlos – SP, 2017, 1-21.

[14] Varshneya A.K., Mauro J.C. Fundamentals of Inorganic Glasses, 3rd edition, Elsevier, 2019.

[15] Fredericci C., Morelli M.R. - Corrosion of AZS and AZ crucibles in contact with a blast-furnace slag-based glass. Materials Research Bulletin 35, 2000, 2503–2514. doi.org/10.1016/S0025-5408(00)00462-1

[16] Marota A., Buri A., Branda F. Heterogeneous bulk nucleation and differential thermal analysis. Journal of Thermal Analysis and Calorimetry, 21, 2, 1981, 227-233. doi.org/10.1007/bf01914205

[17] Zenebe C.G. A Review on the Role of Wollastonite Biomaterial in Bone Tissue Engineering. BioMed Research International, 2022, 1-15. doi.org/10.1155/2022/4996530